Quasielastic light scattering in the one-dimensional superionic conductor hollandites

S. Furusawa, T. Suemoto, and M. Ishigame
Research Institute for Scientific Measurements, Tohoku University, Katahira, Sendai 980, Japan
(Received 27 August 1987; revised manuscript received 15 August 1988)

The wave-vector, polarization, and temperature dependencies of the quasielastic light scattering (QELS) have been studied in the one-dimensional superionic conductor K and Cs hollandite crystals. Based on the wave-vector and the temperature dependencies, the origin of the QELS has been attributed to ionic hopping in a one-dimensional tunnel. The polarization characteristics of the QELS for the K hollandite can be well explained by the "pair diffusion model" applied to a one dimensional ion hopping process. The temperature dependence of the QELS intensity is found to depend drastically on the ionic species. This is well explained in terms of the extended "pair diffusion model," in which the distribution of activation energy for ion hopping is introduced.

I. INTRODUCTION

Superionic conductors have attracted considerable and growing interest not only for the usefulness of the high ionic conductivity, but also from the viewpoint of basic research in solid-state physics. Among the many superionic conductors,[1,2] hollandite is one of the important materials in the basic research of the superionic conductors, since the ion-conduction mechanism is expected to be simple, and the clearcut theoretical treatment could possibly describe the system,[3-10] owing to the one-dimensional (1D) crystal structure.

Hollandite has a chemical formula $A_{2x}M_xTi_{8-x}O_{16}$ (where $A=K^+,Rb^+,Cs^+,Tl^+,\ldots$; $M=Mg^{2+},Zn^{2+},Cu^{2+},\ldots$), belonging to a space group C_{4h}^5 $(I4/m)$.[11-13] A primitive unit cell contains one chemical formula of $A_{2x}M_xTi_{8-x}O_{16}$. Hollandite has tunnels aligned in one direction. The framework is constructed by TiO_6 octahedra, and the A^+ ions are kept in the tunnels formed in the framework. By replacing a part of Ti^{4+} ions by M^{2+} ions, vacancies are introduced on the A^+-ion sites to compensate for the negative charge imposed by this replacement. Thus, A^+ ions can move along the c axis through the vacancy.

During the last decade the 1D characters of mobile ions in hollandite have been studied experimentally with x-ray[13-15] and electron diffraction[12,16] and NMR.[17,18]

From the ac conductivities of hollandite,[19-22] a large difference between conductivities in parallel and perpendicular directions to the c axis is found.[22] From the measurements of the specific heat below 3 K,[23] it is shown that the low-energy excitations due to the ion-ion interactions[4,23,24] play an important role in the dynamics of the ionic diffusion mechanism for hollandite. From the measurements of infrared reflection and Raman scattering for hollandite, the vibrational properties are discussed in relation to the breakdown of the translational symmetry for the crystal.[25-28] In particular, from low-frequency light-scattering measurements the attempt frequencies for Tl^+ and Cs^+ species are determined.[28]

Recently, it has been shown that quasielastic light scattering (QELS) is a very powerful tool in the study of the microscopic ionic diffusion process in superionic conductors.[29-31] Theoretically, Klein derived the frequency dependence of QELS for superionic conductor, assuming that there are several inequivalent sites for mobile ions in a primitive unit cell.[32,33] After that, Dieterich and Peschel proposed the "pair diffusion model," assuming the classical ion-hopping process.[5] In this model they developed the frequency dependence of the QELS spectrum and showed that the intensity of QELS diverges at $\omega=0$ for the 1D ion-hopping process. This singular nature of the QELS for the 1D ion-hopping process is quite different from the results of Klein's treatment. Since this system is considered to be a prototype of a 1D ion conductor, and the mobile ions in hollandite have little interchannel interaction,[7,13-15] it is very interesting to study the behavior of QELS in this material.

In this paper we reveal the origin of QELS observed for hollandite. Furthermore, the polarization characteristics and the temperature dependence of QELS are investigated in detail to clarify the microscopic ion-hopping process for hollandite.

II. EXPERIMENTAL PROCEDURES

K and Cs hollandite ($K_{2x}Mg_xTi_{8-x}O_{16}$, $x=0.8$ and $Cs_{2x}Mg_xTi_{8-x}O_{16}$, $x=0.6$) single crystals have been prepared by a flux method. We describe the procedure of flux method in the case of K hollandite. The reagents used for the crystal growth of Cs hollandite are indicated in parentheses.

(1) High-purity K_2CO_3 (Cs_2CO_3), MgO, and TiO_2 were mechanically mixed in the mole ratio 3:1:3. The mixture was melted in air using a 70-kW large solar furnace to synthesize hollandite.

(2) The mixture of high-purity K_2MoO_4 (Cs_2MoO_4) and MoO_3 in the mole ratio 2:1 was used as a flux.

(3) A 30-ml platinum crucible was loaded with about 90 g flux and 25 g hollandite powder.

(4) The covered crucible was sealed by caulking using a platinum ribbon, and then inserted in an electric furnace. The temperature of the furnace was elevated to 1643 K at a rate of 170 K/h. After the crucible was kept at about

1643 K for 3 h, the furnace was cooled at a rate of 3.5 K/h down to 1193 K and switched off. The flux was dissolved in water.

The single crystals obtained have a needlelike shape with dimensions of about $0.2\times0.2\times10$ mm^3 on the average. The analytical electron microscope was used to characterize the synthesized crystal. The results of the analysis showed that the values of x were 0.80 ± 0.05 and 0.60 ± 0.05 for $K_{2x}Mg_xTi_{8-x}O_{16}$ and $Cs_{2x}Mg_xTi_{8-x}O_{16}$, respectively. The single crystals were cut into a rectangular shape having (100), (010), and (001) faces. All faces of the crystals were polished to give optically smooth surfaces sufficient for use in the light-scattering measurements.

To measure QELS we used a tandem Fabry-Perot interferometer equipped with a grating monochromator. A single-mode oscillation of the 5145.36-Å line from an Ar-ion laser was used as an excitation source. Since the apparatus used here[29,30] is virtually identical to that used by Lyons and Fleury[34] in conjunction with an iodine-vapor filter for the study of very-low-frequency spectra, only a brief description is given for the QELS measurement system. The elastic component of the scattered light was reduced to less than 10^{-7} by the iodine vapor filter,[34] and the scattered light was coarsely dispersed by a grating monochromator having a resolution of 10 cm^{-1}. The "monochromatic" light was then directed into a tandem Fabry-Perot interferometer, which consists of two single-pass Fabry-Perot interferometers having free spectral ranges of 9.7 and 1.45 cm^{-1}, respectively. The finesse of each interferometer was about 50. Each of two interferometers was set in the airtight box, which was connected to a common pressure buffer. The frequency was scanned by varying the pressure of freon gas in the box. The scanning of the interferometers and the drive of the grating monochromator were controlled synchronously by a microcomputer.

With this system, the interferences of different orders, which appear with an interval of 29.1 cm^{-1}, were unambiguously eliminated to give strictly one frequency free from any stray light. The resolution of the total system was 0.03 cm^{-1}. The signal was recorded by a single-photon-counting method. The samples were heated by an electric furnace or cooled by a liquid-nitrogen cryostat in vacuum.

III. RESULTS AND DISCUSSION

A. Polarization characteristics of QELS

In general, the QELS spectrum appears upon Rayleigh scattering with a peak at wave-number shift 0 cm^{-1}. Figure 1 shows the observed QELS spectrum of K hollandite, which is measured in a right-angle scattering geometry with the polarization $X(Z,Z)Y$ at room temperature. Here, an orthogonal Cartesian coordinate system X,Y,Z is set with the Z axis parallel to the crystal c axis and the X and Y axes parallel to the other two crystal axes. In this figure the spectrum is strongly deformed by the structured transmission efficiency of the iodine-vapor filter. Furthermore, the scattering intensity in the

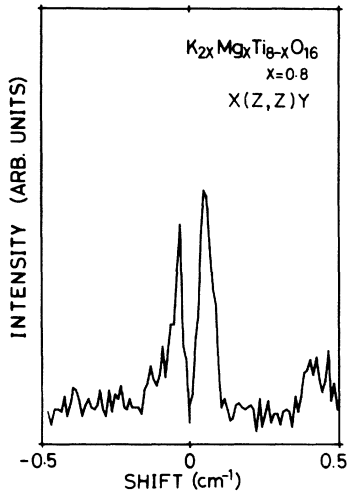

FIG. 1. QELS spectrum for K hollandite at room temperature, which is greatly deformed by the structured transmission efficiency of the iodine-vapor filter.

frequency region inside ±0.03 cm^{-1} is completely masked by the absorption of iodine vapor. In order to estimate the half-width of the spectrum, we reconstructed the true spectrum from this curve by normalizing it using a transmission spectrum of the iodine-vapor filter. If we try to fit the reconstructed spectrum by a Lorentzian, the half-width will be approximately 0.1 cm^{-1}.

In the mechanism of QELS in solids, various origins are known; that is, ion hopping,[5,29–33] fluctuation of density in the heat-conduction process,[35,36] structural phase transitions,[37] and the two-phonon-difference process in second-order Raman scattering.[38–42] In the case of QELS, due to the heat-conduction process the half-width should be proportional to the square of the wave-vector transfer. However, from our measurement the value of the half-width does not show a scattering-angle dependence for 5°, 90°, and 180°. Therefore, the heat-conduction process is unlikely to be responsible for the observed QELS. Furthermore, from the value of half-width it is not plausible to ascribe the observed QELS to the second-order Raman effect arising from the two-phonon-difference process, since the two-phonon-difference band extends usually to several cm^{-1}.[41] From these facts, the observed QELS is considered to be due to ion hopping in hollandite crystal.

The polarization characteristics of QELS due to ion hopping are very useful to understand the hopping mechanism, because the Raman-scattering tensor of QELS is closely related to the ion-hopping processes. In order to determine the Raman tensor of QELS, we measured the spectra in several different scattering geometries and polarizations. Since the superradiance of the Ar-ion laser might spoil the measurement in the very-low-frequency region, we have taken special caution against the fluorescence from the laser throughout the series of experiments. In the backscattering geometry, we eliminated the bright spot on the front surface of the sample from the entrance slit of the premonochromator by tilting the laser beam by about 5°. We also used a small pinhole just

before the laser collimating lens to remove divergent light from the laser. By using these two precautions, we were able to obtain reliable spectra free from an influence of fluorescence of the laser plasma. Furthermore, we have made a more severe test to exclude the possibility of fluorescence: Instead of the sample, we placed a piece of ceramic which gave Rayleigh scattering about 10^4 times larger. In this case, the intensity of the fluorescence was about 10–20 counts/s. By dividing the intensity of the fluorescence by 10^4, we estimated the contribution of the fluorescence in the QELS measurements to be about 10^{-3} counts/s. This count rate is negligibly small compared to the QELS intensity in K and Cs hollandites (3–7 counts/s). In Figs. 2 and 3 the observed QELS spectra at 300 K are shown. The integrated intensity of each spectrum is estimated after subtracting dark counts. The results are shown in the following matrix form after normalizing each component, assuming that the integrated intensity in polarization component $X(Z,Z)Y$ is equal to that in $\bar{Y}(Z,Z)Y$:

$$\begin{bmatrix} 61 & 2 & 4 \\ 2 & 61 & 4 \\ 4 & 4 & 100 \end{bmatrix} . \quad (1)$$

In this matrix it is seen that only the diagonal components have large values compared with the off-diagonal components. Neglecting the small values of the off-diagonal components, this matrix is found to correspond to a squared Raman tensor with the symmetry of A_g in the point group C_{4h}.

In the Klein's treatment,[32,33] it is assumed that there are several inequivalent sites for mobile ions in a primitive unit cell. In the case of hollandite, each primitive unit cell includes two 1D ion-hopping channels. Since mobile ions cannot hop perpendicular to the c axis, it will be appropriate to consider the ion hopping only in a single channel for hollandite. As the single-ion channel has only one mobile-ion site in a primitive unit cell, all of the mobile-ion sites in the single channel are considered to be equivalent by translational symmetry. Therefore, it is difficult to understand the observation of QELS in hollandite from Klein's point of view.

On the other hand, the creation and annihilation of the ion pair are possible in hollandite crystal. In the pair diffusion model proposed by Dieterich and Peschel,[5] it is assumed that the polarizability of the ions changes when they make a "pair," which means simultaneous occupation of the adjacent two sites by two ions. When the ions hop from one site to the other site, the pair will be created or annihilated, leading to polarizability fluctuation, which induces QELS.

The contribution to the polarizability tensor from pairs is given by the following equation,[5]

$$\alpha_{\mu\nu}=\tfrac{1}{2}\sum_{l,\delta}[(\alpha_{\parallel}+2\alpha_{\perp})\delta_{\mu\nu}/3+(\alpha_{\parallel}-\alpha_{\perp})(\delta_{\mu}\delta_{\nu}-\delta_{\mu\nu}/3)]n_l(t)n_{l+\delta}(t) , \quad (2)$$

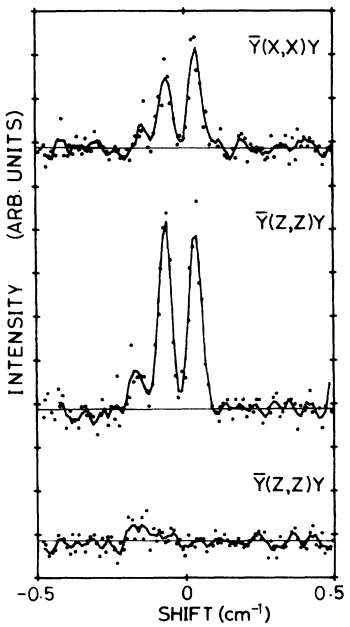

FIG. 2. Polarized QELS spectra in K hollandite at room temperature measured in backscattering configurations $\bar{Y}(X,X)Y$, $\bar{Y}(Z,Z)Y$, and $\bar{Y}(Z,X)Y$ by using an iodine-vapor filter. A horizontal baseline for each spectrum is the dark-count level.

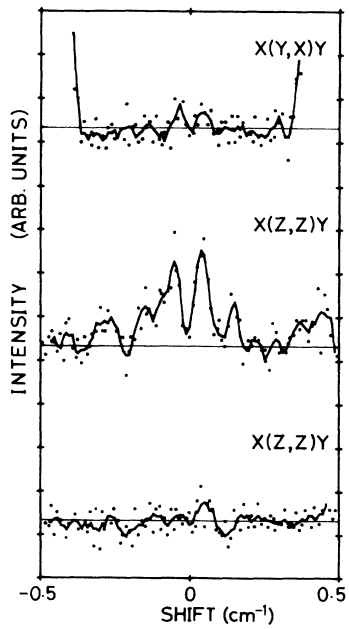

FIG. 3. Polarized QELS spectra in K hollandite at room temperature measured in right-angle-scattering configurations $X(Y,X)Y$, $X(Z,Z)Y$, and $X(Z,X)Y$ by using an iodine-vapor filter. A horizontal baseline for each spectrum is the dark-count level.

where $\alpha_{\parallel}$ and $\alpha_{\perp}$ are the polarizability components of a pair, which are parallel and perpendicular to the pair axis, respectively. l denotes the site and $l+\delta$ denotes the nearest-neighbor site of site l. δ_{μ} and δ_{ν} are components of a unit vector which is parallel to the pair orientation. $\delta_{\mu\nu}$ is a Kronecker delta. The function $n_l(t)$ is the average occupation number of site l at time t for a given initial particle distribution $n_l(0)$ at $t=0$.

Since the orientation of the pair is always parallel to the c axis in this case, the polarizability tensor is written in following matrix form,

$$\alpha=\frac{1}{2}\begin{bmatrix}\alpha_{\perp} & & \\ & \alpha_{\perp} & \\ & & \alpha_{\parallel}\end{bmatrix}\sum_{l,\delta} n_l(t)n_{l+\delta}(t) \ . \tag{3}$$

Equation (3) is just the same form as the matrix form given by Eq. (1) obtained by our experiment. Thus, the polarization characteristics of the QELS intensity in K hollandite can be well explained by the pair diffusion model applied to the one-dimensional ion-hopping process.

B. Temperature dependence of QELS

We have measured the temperature dependence of the QELS intensity at fixed frequency 0.05 cm^{-1} for K and Cs hollandites through a frequency window with a width of 0.03 cm^{-1}, which corresponded to the resolution of the interferometers. This method has an advantage over the usual spectrum measurement in studying the ionic diffusion process, that is, when the QELS intensity is measured at a fixed frequency as a function of temperature, the correction for the absorption spectrum of iodine-vapor filter is not necessary to estimate the value of Γ.

The results are shown in Figs. 4 and 5 (solid circles). Here, the experimental data points were smoothed by the least-squares method using a polynomial. The temperature dependence of the QELS intensity for Cs hollandite has a maximum around 420 K, as seen from Fig. 5. On the other hand, the QELS intensity for K hollandite in Fig. 4 shows very weak temperature dependence, where a maximum of QELS intensity seems to appear around 125 K.

As mentioned in subsection A, polarization characteristics of the QELS intensity in hollandite crystal have been understood by the pair diffusion model. Therefore, we have analyzed the temperature dependence of the QELS intensity by using the same model.

In this model, the time correlation function $\langle \alpha_{\mu\nu}(t)\alpha_{\mu\nu}(0)\rangle$ can be written as

$$\langle \alpha_{\mu\nu}(t)\alpha_{\mu\nu}(0)\rangle \propto \sum_{l,l'}\sum_{\delta,\delta'}\langle n_l(t)n_{l+\delta}(t)n_{l'}(0)n_{l'+\delta'}(0)\rangle \ . \tag{4}$$

Here, the time development of $n_l(t)$ in Eq. (4) can be described by the following equation;

$$\frac{d}{dt}n_l(t)=\sum_{\delta}\Gamma[n_{l+\delta}(1-n_l)-n_l(1-n_{l+\delta})](t) \ . \tag{5}$$

Here, Γ is the hopping rate of the ions. This equation means that the time development of occupation number at site l is given by the difference of the hopping number from site $l+\delta$ to site l and from site l to site $l+\delta$. Then, the equation of motion for pairs $n_{l'}(t)n_{l'+\delta}(t)$ is given as follows,

$$\frac{d}{dt}[n_{l'}n_{l'+\delta}(t)]=\Gamma\left[\sum_{\delta'\neq\delta}(n_{l'+\delta'}-n_{l'})n_{l'+\delta}+\sum_{\delta'\neq-\delta}n_{l'}(n_{l'+\delta+\delta'}-n_{l'+\delta})\right] \ . \tag{6}$$

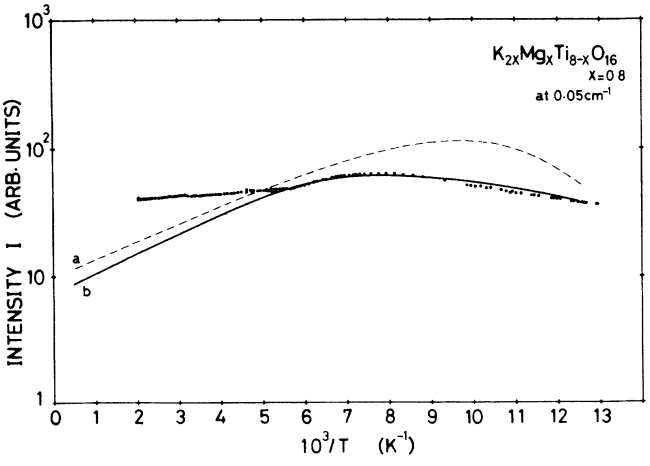

FIG. 4. Temperature dependence of the QELS intensity in K hollandite measured at a frequency shift 0.05 cm^{-1}. The dashed curve a represents the one calculated by using Eq. (8). The solid curve b shows the one calculated by using Eq. (14).

Using a Green's-function technique, Dieterich and Peschel give an analytical solution of Eq. (6) for one-dimensional ion hopping as follows,[5]

$$D_{1,1}(q,Z)=\frac{1}{4\Gamma}\frac{[Z(Z+8\Gamma)+16\Gamma^2\sin^2(q/2)]^{1/2}-Z}{Z+2\Gamma\sin^2(q/2)} \ . \tag{7}$$

Here, $D_{1,1}(q,Z)$ is the pair propagator in one dimension, q is the wave vector, and Z is $-i\omega$. Then, the spectrum is given by $\mathrm{Re}D_{1,1}(q,-i\omega)$. For $q=0$, $\mathrm{Re}D_{1,1}(0,-i\omega)$, which represents the frequency dependence of QELS, can be easily deduced as follows,

$$I(\omega)=\frac{I_0}{4\Gamma}\left[\left[\frac{1+[1+(8\Gamma/\omega)^2]^{1/2}}{2}\right]^{1/2}-1\right] \ . \tag{8}$$

To calculate the temperature dependence of the QELS intensity, the hopping rate of the ions is assumed to have a simple form of activation type, as follows,

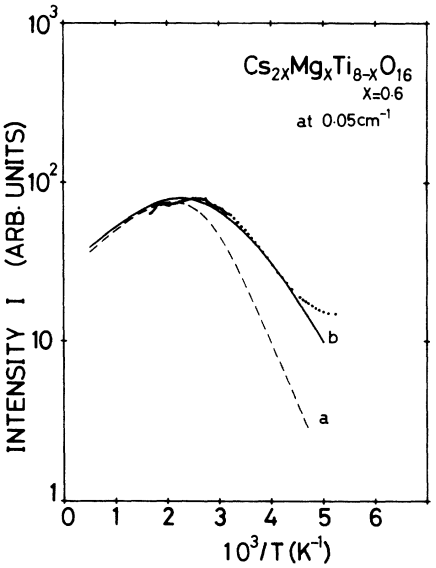

FIG. 5. Temperature dependence of the QELS intensity in Cs hollandite measured at a frequency shift 0.05 cm^{-1}. The dashed curve *a* represents the one calculated by using Eq. (8). The solid curve *b* shows the one calculated by using Eq. (14).

$$\Gamma=\Gamma_0\exp(-\Delta/k_BT) . \tag{9}$$

Here, Γ_0 is the attempt frequency and Δ is the activation energy of the ions.

As discussed by Dieterich and Peschel, the pair propagator $D_{1,1}(0,Z)$ diverges for $Z\rightarrow 0$ and the spectrum diverges as $(1/\omega)^{1/2}$ for $\omega\rightarrow 0$, reflecting the singular nature of the spectrum in one dimension. Furthermore, it is easily shown that when $\ln I(\omega)$ is plotted as a function of $1/T$, the temperature dependence of $\ln I(\omega)$ shows a maximum at a characteristic temperature

$$T_{\max}=-\Delta/k_B\ln[(2+\sqrt{5})^{1/2}(\omega/\Gamma_0)/4] ,$$

where a relation $\Gamma=[(2+\sqrt{5})^{1/2}/4]\omega$ holds between Γ and ω. The slope of $\ln I(\omega)$ is then given by $\Delta/2k_B$ at extremely high temperatures above $T_{\max}$, while the slope of the $\ln I(\omega)$ is given by $-\Delta/k_B$ at extremely low temperatures below $T_{\max}$.

To evaluate the temperature dependence using Eqs. (8) and (9), the values of Δ and Γ_0 are necessary. The ionic conductivity σ can be related to the diffusion coefficient through the Nernst-Einstein relation as

$$\sigma=\frac{N_v(Ze)^2}{k_BT}D . \tag{10}$$

Here, Ze is the charge of the carrier, N_v is the number of carriers, and D is the diffusion coefficient of the hopping ions, which is given by a random-walk model in the 1D case as

$$D=(a_0^2/2)f . \tag{11}$$

Here, a_0 is the hopping distance and f is a correlation factor of the order of 1. Then, the ionic conductivity σ is given as follows,

$$\sigma=\frac{N_v(Ze)^2a_0^2}{2k_BT}f\Gamma_0\exp\left[-\frac{\Delta}{k_BT}\right] . \tag{12}$$

As the value of σ is strongly frequency dependent, we have to use a value at 1.5 GHz corresponding to the frequency of observation in QELS. For Cs hollandite, the values of Δ and Γ_0 are estimated from the conductivity data at 1.5 GHz (Ref. 43) using Eq. (12). For K hollandite, on the other hand, the values of Δ and Γ_0 are estimated from the conductivity data at 30 GHz (Ref. 21) using Eq. (12) because no conductivity data at 1.5 GHz are available. The estimated values of Γ_0 and Δ for Cs and K hollandite are listed in Table I, together with the reported values of $\sigma(T)$.[21,43]

Using the estimated values of Γ_0 and Δ, the intensity of QELS at $\omega=0.05$ cm^{-1} is calculated from Eqs. (8) and (9). The results are shown by dashed curves (*a*) in Figs. 4 and 5 for K and Cs hollandites, respectively. This simple model can explain two remarkable behaviors of the temperature dependence. First, the temperature of the intensity maximum is higher for Cs hollandite than for K hollandite. Secondly, the temperature dependence is more pronounced in Cs hollandite than in K hollandite. These behaviors can be qualitatively understood in terms of the difference in the activation energy of the ion hopping. However, it is seen from these figures that the shape of the calculated curves does not agree with the experimental results. This fact suggests the existence of distribution in the hopping rate Γ. The distribution of Γ for hollandite has been already suggested by Beyeler *et al.*[44] They have proposed an exponential-type distribution function to explain the frequency dependence of the ionic conductivity of hollandite in the frequency region 10^2–10^7 Hz,

TABLE I. Values of parameters which are used for the numerical calculation of Eqs. (8), (12), and (14).

	Parameter							
Sample	σ (Ω/cm)	T (K)	N_v (cm^{-3})	Δ (eV)	Γ_0 (Hz)	T_m (K)	Δ_l (eV)	Δ_h (eV)
$K_{2x}Mg_xTi_{8-x}O_{16}$ ($x=0.08$)	0.40	160	1.52×10^{21}	0.058	3.2×10^{12}	508	0.04	0.10
$Cs_{2x}Mg_xTi_{8-x}O_{16}$ ($x=0.6$)	0.0045	284	2.60×10^{21}	0.15	0.19×10^{12}	850	0.10	0.19

while a Gaussian distribution function of the relaxation time has been proposed in the case of other superionic conductors, for example, β-alumina[45] and yttria-stabilized zirconia.[29,31] In this paper, we use the exponential-type distribution function $P(\Delta)$ introduced by Beyeler *et al.*[44] According to Beyeler's treatments, $P(\Delta)$ is given as follows,

$$P(\Delta)=P_0\exp(-\Delta/k_BT_m) . \quad (13)$$

Here, T_m is a mobility transition temperature which determines the distribution of activation energy.

The QELS spectrum $S(\omega,t)$ can be represented by an integral form,

$$S(\omega,T)=\int_{\Delta_l}^{\Delta_h} P(\Delta)I(\omega,T,\Delta)d\Delta . \quad (14)$$

Here, the function $I(\omega,T,\Delta)$ is defined by Eqs. (8) and (9). Δ_h and Δ_l are upper and lower limits of activation-energy distribution, respectively. In calculating Eq. (14), we used the values of Γ_0 and T_m given in Table I, which have been reported by Yoshikado *et al.*[18,43] Δ_h and Δ_l were used as adjustable parameters.

When the values of Δ_h and Δ_l given in Table I are used, the observed temperature dependence of QELS can be well fitted by the curves of $S(\omega,T)$ calculated from Eq. (14) for Cs hollandite (Fig. 5, curve *b*). For K hollandite, the calculated curve $S(\omega,T)$ gives good agreement with the experimental curve below 195 K.

This distribution in the hopping rate Γ is also used to understand the line shape. In order to compare the expected spectrum with the experimental results, we simulated a spectrum, which should be observed through the iodine-vapor filter, by using a "true spectrum" calculated from Eq. (14) with the parameters indicated in Table I. In this calculation we used the transmission spectrum of the iodine-vapor filter measured under the same conditions as in Fig. 3, by using a tungsten lamp as a light source. As shown in Fig. 6(a), the simulated spectrum is fairly good agreement with the observed $X(Z,Z)Y$ spectrum. However, the peak is more pronounced for the $X(Z,Z)Y$ spectrum in Fig. 1 and the $\bar{Y}(Z,Z)Y$ spectrum in Fig. 2. This discrepancy in the observed shape of the tail is not ascribed to the wave-vector dependence. It is experimentally confirmed that the shape of the tail depends on the position of the sample, in contrast to the good reproducibility of the main feature around 1 GHz. Such a situation might be possible if the barrier-height distribution is not homogeneous through the sample. From Eq. (8), the QELS intensity should be proportional to $\omega^{-1/2}$ in the low-frequency limit and to ω^{-2} in the high-frequency limit. If there are high barriers, the shape of the spectrum becomes more like ω^{-2} rather than $\omega^{-1/2}$. As an example, we show a simulated curve in Fig. 6(b) for $\Delta=0.17$ eV, which is 0.07 eV higher than the upper limit of the above-mentioned distribution. This simulation gives a shape with a pronounced peak and a small tail, which reproduces the observed spectral shape taken in $X(Z,Z)Y$ geometry.

The distribution of activation energy introduced above can be understood as follows. The intrinsic barrier, which is formed by the crystal structure itself, has equal

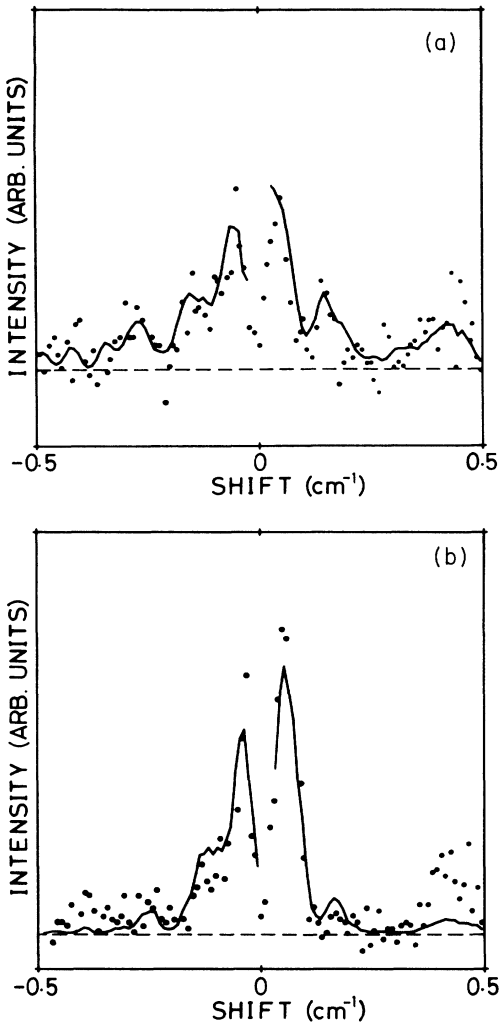

FIG. 6. (a) Solid curve indicates the simulated spectrum for K hollandite at 300 K (see text). The dots represent the $X(Z,Z)Y$ spectrum reproduced from Fig. 3. Dashed line indicates the dark-count level. (b) Solid curve indicates the simulated spectrum for K hollandite at 300 K (see text). The dots represent the $X(Z,Z)Y$ spectrum reproduced from Fig. 1. Dashed line indicates the dark-count level.

barrier height. However, there are randomly distributed additional higher-energy barriers, called extrinsic barriers, which are formed by defects or impurity atoms in tunnels. Such extrinsic barriers are responsible for the high-activation-energy part of the distribution. On the other hand, a collective excitation caused by ion-ion interactions[4,6,24,46] will contribute the low-activation-energy part of the distribution.

III. CONCLUSIONS

In conclusion, we have observed QELS in 1D superionic conductor K and Cs hollandites, and revealed that the origin of QELS is ion hopping in the 1D tunnel. The main results and interpretations can be summarized as follows.

(1) The polarization characteristics of QELS in K hollandite can be explained in terms of the pair diffusion

model assuming 1D ion hopping.

(2) The temperature dependence of the QELS intensity depends drastically on the hopping-ion species and shows a maximum typical for the ionic conductors.

(3) The temperature dependence of QELS in hollandite crystals is well explained by introducing a distribution of the activation energy, which has been obtained from ac conductivity.

ACKNOWLEDGMENT

The authors wish to thank Dr. H. Arashi and Mr. A. Kaimai for help with the synthesis of hollandites, and Dr. S. Yoshikado for providing us with the conductivity data of Cs hollandite. This work is partly supported by a Grant-in-Aid for Special Project Research from The Ministry of Education, Science and Culture (Japan).

[1]M. Ishigame and T. Suemoto, Zirc. Ceram. **2**, 93 (1984).
[2]G. Lucazeau, Solid State Ionics **8**, 1 (1983).
[3]S. Alexander, Phys. Rev. **23**, 2951 (1981).
[4]L. Pietronero and S. Strässler, Phys. Rev. Lett. **42**, 188 (1979).
[5]W. Dieterich and I. Peschel, J. Phys. C **16**, 3841 (1983).
[6]H. U. Beyeler, L. Pietronero, and S. Strässler, Phys. Rev. B **22**, 2988 (1980).
[7]H. U. Beyeler, L. Pietronero, and S. Strässler, Phys. Rev. Lett. **38**, 1532 (1977).
[8]S. Alexander, J. Bernasconi, W. R. Schneider, and R. Orbach, Rev. Mod. Phys. **53**, 175 (1981).
[9]J. Bernasconi, W. R. Schneider, and W. Wyss, Z. Phys. B **37**, 175 (1980).
[10]P. M. Richards, Phys. Rev. B **16**, 1393 (1977).
[11]J. M. Réau, C. Delmas, and P. Haugenmuller, in *Solid Electrolytes*, edited by Paul Haugenmuller and W. van Gool (Academic, New York, 1978), p. 381.
[12]J. S. Dryden and A. D. Wadsley, Trans. Faraday Soc. **54**, 1574 (1958).
[13]H. U. Beyeler and C. Schüler, Solid State Ionics **1**, 77 (1980).
[14]H. P. Weber and H. Schulz, Solid State Ionics **9&10**, 1337 (1983).
[15]H. U. Beyeler, Phys. Rev. Lett. **37**, 1557 (1976).
[16]A. Pring, D. J. Smith, and D. A. Jefferson, J. Solid State Chem. **46**, 819 (1979).
[17]Y. Onoda, Y. Fujiki, S. Yoshikado, T. Ohachi, and I. Taniguchi, Solid State Ionics **9&10**, 1311 (1983).
[18]Y. Onoda, Y. Fujiki, M. Takigawa, H. Yasuoka, S. Yoshikado, T. Ohachi, and I. Taniguchi, Solid State Ionics **17**, 127 (1985).
[19]H. U. Beyeler and S. Strässler, Phys. Rev. B **24**, 2121 (1981).
[20]S. K. Khanna, G. Grüner, R. Orbach, and H. U. Beyeler, Phys. Rev. Lett. **47**, 255 (1981).
[21]S. Yoshikado, T. Ohach, and I. Taniguchi, Solid State Ionics **7**, 335 (1982).
[22]H. P. Wever and H. Schulz, J. Chem. Phys. **85**, 475 (1986).
[23]H. v. Löhneysen, H. J. Schink, W. Arnold, H. U. Beyeler, L. Pietronero, and S. Strässler, Phys. Rev. Lett. **46**, 1213 (1981).
[24]L. Pietronero and S. Strässler, Solid State Commun. **27**, 1041 (1978).
[25]T. Osaka, Y. Shibata, K. Ishi, and S. Takahashi, Solid State Commun. **55**, 1119 (1985).
[26]T. Ohsaka and Y. Fujiki, Solid State Commun. **44**, 1325 (1982).
[27]M. Ishii, Y. Fujiki, and T. Osaka, Solid State Commun. **55**, 1123 (1985).
[28]Y. Shibata, T. Suemoto, and M. Ishigame, Phys. Status Solidi B **134**, 110 (1986).
[29]T. Suemoto and M. Ishigame, Phys. Rev. B **33**, 2757 (1986).
[30]T. Suemoto, M. Ishigame, T. Sasaki, and K. Minegishi, Bull. Res. Inst. Sci. Meas., Tohoku Univ. **33**, 55 (1985).
[31]T. Suemoto and M. Ishigame, Solid State Commun. **45**, 641 (1983).
[32]M. V. Klein, in *Light Scattering in Solids*, edited by M. Balkanski (Wiley, New York, 1976), p. 351.
[33]R. A. Field, D. A. Gallagher, and M. V. Klein, Phys. Rev. B **18**, 2995 (1978).
[34]K. B. Lyons and P. A. Fleury, J. Appl. Phys. **47**, 4898 (1976).
[35]B. J. Berne and R. Pecora, *Dynamic Light Scattering* (Wiley, New York, 1976).
[36]K. B. Lyons and P. A. Fleury, Phys. Rev. Lett. **37**, 161 (1976).
[37]A. D. Bruce and R. A. Cowley, Adv. Phys. **29**, 219 (1980).
[38]J. Jäckle, in *Amorphous Solids*, edited by W. A. Phillips (Springer-Verlag, Berlin, 1981), p. 135.
[39]M. Cardona, in *Light Scattering in Solids II*, edited by M. Cardona and G. Guntherödt (Springer-Verlag, Berlin, 1982), p. 19.
[40]I. P. Ipatova, A. A. Maradudin, and R. F. Wallis, Fiz. Tverd. Tela (Leningrad) **8**, 1064 (1966) [Sov. Phys.—Solid State **8**, 850 (1966)].
[41]I. P. Ipatova, A. A. Maradudin, and R. F. Wallis, Phys. Rev. **155**, 882 (1967).
[42]K. B. Lyons, P. A. Fleury, and H. L. Carter, Phys. Rev. B **21**, 1653 (1980).
[43]S. Yoshikado (private communication).
[44]R. E. Walstedt, R. Dupreee, J. P. Remeika, and A. Rodriguez, Phys. Rev. B **15**, 3442 (1977).
[45]J. Bernasconi, H. U. Beyeler, S. Strässler, and S. Alexander, Phys. Rev. Lett. **42**, 819 (1979).
[46]L. Pietronero, W. R. Schneider, and S. Strässler, Phys. Rev. B **24**, 2187 (1981).